

# **Resonant Attachment Method for Trace Oxygen Detection**

Kin F. Man, Saïd Boumsellek and Ara Chutjian

Jet Propulsion Laboratory  
California Institute of Technology  
4800 Oak Grove Drive  
Pasadena, CA 91109

A Paper to the

6th International Symposium:  
Experimental Methods for Microgravity Materials Science

1994 Annual TMS Meeting  
San Francisco, CA  
Feb 27- Mar 3, 1994

## Abstract

A technique for detecting trace quantities of oxygen has been developed. It utilizes the resonant electron dissociative attachment process where the electron attachment cross section for the  $e^- - O_2$  interaction to form  $O^-$  ions is greatly enhanced at the resonant energy (6.8 eV). A small gridded electron ionizer has been shown to be highly sensitive for measuring low concentrations of  $O_2$  in  $N_2$  using the method of standard additions. The lowest detection limit obtained was 1.2 kHz ( $O^-$  count rate) at a concentration of  $10^{-10}$  (0.1 ppb).

## 1. Introduction

Gaseous contaminants such as oxygen, water vapor, nitrogen and hydrocarbons are often present in the processing/<sup>f</sup> abdication chamber in containerless materials processing or semiconductor device fabrication. The processes encompass crystal growth, semiconductor fabrication, pharmaceutical manufacture, materials purification, etc. The contaminants arise as a result of outgassing from hot surfaces or they may be part of the impurities in the buffer gas (even in commercial ultra-high purity gases). Among these gaseous contaminants, oxygen is the most reactive and, therefore, has the most adverse effects on the operations. It can lead to rapid surface oxide formation, hence affecting the quality of semiconductor devices; or it can become an unwanted nucleation source in undercooking experiments. A simple calculation [1] shows that if the concentration of oxygen in a processing chamber at 1000 °C is in the parts-per-billion (ppb) level, it will only take about 10 seconds for an oxide layer to form on the surface of a sample.

Controlling and monitoring the oxygen level in the chamber environment is therefore crucial to the success of containerless processing experiments and semiconductor device fabrication. At the Jet Propulsion Laboratory, there is an intense effort to develop different types of oxygen sorbents [2,3,4] to reduce oxygen concentration in processing chambers to sub-ppb level. It is necessary to have an instrument that can measure concentrations down to these low levels. Unfortunately, such low concentration levels are extremely difficult to measure.

Most commercial instruments for trace oxygen measurement use an electrochemical cell as the sensor element. Solid electrolytic detectors generally have an oxygen detection limit of around 50 ppb and liquid electrolytic detectors generally have a slightly lower limit. While the Atmospheric Pressure Ionization Mass Spectrometer (API MS) has a potential of measuring below one ppb level for some gas species, it has not been tested for oxygen.

This paper describes a new technique for measuring trace oxygen contaminants that utilizes the resonant electron attachment method. This method exploits the fact that the electron dissociative attachment cross section is greatly enhanced at the resonance energy, giving a much higher detection sensitivity; therefore enabling lower concentrations to be measured. An experimental setup

(based on the READ instrument [5,6,7]) used to demonstrate this method is also described and the results presented.

## 2. Resonant Attachment Method

The resonant attachment method is based on electron attachment at the resonance energy, followed by mass detection of the negative ion species. This technique utilizes the well-known fact that the attachment cross section is greatly enhanced at the resonance energy.

Two principal modes of electron attachment (dissociative and nondissociative) are possible with the bombardment of a molecule, denoted by AB, by resonant-energy electrons:

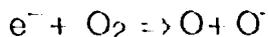


and



In nondissociative electron attachment the parent negative ions formed are normally stable with respect to dissociation and auto-detachment. The parent ions are then detected, allowing unambiguous determination of the molecular species. In dissociative electron attachment the parent molecules are inferred from detection of the product ions, B<sup>-</sup> in this example.

For molecular oxygen, the dissociative electron attachment process is as follows :



The resonance energy for O<sup>-</sup> formation by electron impact of molecular oxygen is 6.8 eV (figure 1) with a cross section of  $1.34 \times 10^{-18} \text{ cm}^2$  [8, 9]. The detection of O<sup>-</sup>, in this case, is used as signature for the presence of the contaminant molecular oxygen.

### 3. Sensitivity Calculation for O<sup>-</sup> Detection from O<sub>2</sub>

In order to evaluate the capability of this technique and to obtain an estimate of its detection limit, we have conducted a calculation based on realistic experimental parameters. The detected O<sup>-</sup> signal count rate, S (in Hz), from electron attachment to O<sub>2</sub> (in single collision conditions) at the resonance energy is given by:

$$S(\text{Hz}) = \kappa \cdot n_T \cdot V \cdot n_e \cdot v_e \cdot \sigma(E) \quad (\text{eqn. 1})$$

where

**E** is the electron energy, at the resonant dissociative attachment energy of oxygen, = 6.8 eV.

$\sigma(E)$  is the cross section for O<sup>-</sup> production at the resonance energy, =  $1.34 \times 10^{-18} \text{ cm}^2$ .

$v_e$  is the electron velocity at the resonance energy (6.8 eV) =  $14.8 \times 10^7 \text{ cm} \cdot \text{s}^{-1}$ .

$n_e$  is the electron density, estimated to be  $2.6 \times 10^8 \text{ cm}^{-3}$  for a 50  $\mu\text{A}$  beam.

V is the size of the collision region which is a spherical volume<sup>6</sup>, estimated to be  $2 \times 10^2 \text{ cm}^3$ .

$n$ , is the molecular oxygen density at room temperature, a quantity to be determined.

$\kappa$  is the transmission coefficient corresponding to the quadruple mass efficiency and the loss of ions during extraction, estimated to be 0.005. This includes the 50% duty cycle, which is necessary for the operation of the device (see Section 4).

Assuming a signal rate of 100 Hz is necessary for a reasonable signal-to-noise ratio one may calculate from equation 1 the corresponding value of  $n_T$  in the atmosphere to be detected:

$$n_T = 1.73 \times 10^7 \text{ cm}^{-3}$$

This corresponds to a fractional concentration in air of:

$$C = 0.67 \times 10^{-12}$$

This calculation shows that it is capable, theoretically, of detecting concentrations in the sub-ppt level.

#### 4. Experimental Demonstration

A schematic diagram of the experimental setup is shown in figure 2. Electrons are produced at the filaments, F, and are accelerated through a cylindrical grid, G. Within G is an electrically-isolated stainless steel tube, T, which is perforated with several rows of small holes to allow the oxygen molecules to effuse through.

Potentials on F, G and T are arranged so that electrons from F are accelerated towards G, then decelerated and reflected near the surface T. Around this reversal region electrons have a range of energies from nearly zero to several eV, depending on the potentials. Electron collisions with the target gas species effusing through T at the appropriate energy (6.8 eV in this case) lead to the process of dissociative electron attachment of the oxygen gas. The resulting negative ions,  $O^-$ , are extracted along the length T by the extraction cone EC and lens  $L_1$ . Ions are focused with a three-element lens system,  $L_1$ ,  $L_2$ , and  $L_3$ , onto the entrance aperture A of a quadrupole mass analyzer (QMA). They are detected with a channel multiplier (CM), amplified (AMP), and counted by a single-channel scaler with a variable integration time.

The electron acceleration and ion extraction are operated in a pulsed mode (with 50% duty cycle) at a repetition rate of 9 kHz. During the 'electrons ON' cycle, a 12 V potential is applied to G. Electrons from F are accelerated through G towards the grounded T and attach to oxygen molecules effusing through T. In this phase the voltages on elements EC and  $L_1$  are held at ground so that penetrating fields from these elements do not interfere with fields in the collision region and hence do not distort the motion of the low energy electrons. During the 'electrons OFF and ions ON' cycle the voltage at the grid is reduced to -0.05 V and the voltages on EC and  $L_1$  are both raised to 50 V.  $L_2$  and  $L_3$  are set to 170 V and 40 V respectively to extract the  $O^-$  ions from the collision region.

A mass spectrum corresponding to the negative ions formed in dissociative electron attachment of  $O_2$  is shown in figure 3. A peak is clearly visible at  $m/e=16$  corresponding to  $O^-$ . To determine the analytical capability of this technique, a

sensitivity curve was obtained using the method of standard additions [10]. Mixtures of  $O_2$  in  $N_2$  (99.99% purity) were prepared at various fractional concentrations,  $C$  (by particle density) from 1.0 (pure  $O_2$ ) to  $1 \times 10^{-10}$ , in a stainless steel vacuum system. All lines were thoroughly outgassed to prevent contamination of the mixtures during preparation and transferred to the target region which was kept at  $2 \times 10^{-7}$  torr pressure.

The  $O^-$  signal was measured as a function of  $C$  and the sensitivity obtained from the slope of the standard-additions plot. These results are shown in figure 4. Errors in the data represent the quadrature sum of the statistical counting error, and the error in reading the pressure gauges used to make up each fraction. They are given at the 1.70 (90%) confidence level. The  $O^-$  signal,  $S$ (Hz), has a maximum value  $S=21$  kHz in the pure case ( $C=1$ ) then decreases uniformly to a value of  $S=1.2$  kHz at  $C=1 \times 10^{-10}$  (0.1 ppb). Below this concentration, the signal began to fluctuate and a stable reading was not obtained. However, the sensitivity could be substantially improved with increased electron currents and improved ion extraction optics.

## 5. Acknowledgments

This work was carried out at the Jet Propulsion Laboratory, California Institute of Technology, under contract with the National Aeronautics and Space Administration (NASA). It was partly supported by the Federal Aviation Administration Technical Center through agreement with NASA.

## 6. References

1. F. K. Sharma, 4th Int. Conf. on 'Experimental Methods for Microgravity Materials Science Research', Ed. R. A. Schiffman, A Publication of the Minerals, Metals & materials Society, Warrendale, Pennsylvania 127-132 (1992)
2. P. K. Sharma and P. K. Seshan, Chemically Modified Oxide Surfaces, Vol. 3. Eds. D.E. Leyden and W. T. Collins, Gordon and Breach, New York, 65-80 (1990)
3. P. K. Sharma and P. K. Seshan, "Copper Modified Carbon Molecular Sieves for Selective Oxygen Removal," U.S. Patent #/ 5,081,097 (1992)

4. P. K. Sharma and P. K. Seshan, Gas Separation and Purification 4203 (1990)
5. M. T. Bernius and A. Chutjian, Rev. Sci.Instrum. 60779 (1989)
6. S. Boumsellek and A. Chutjian, Anal. Chem.Instrum. 642096 (1992)
7. S. Boumsellek and A. Chutjian, Rev. Sci.Instrum. 64, 1135 (1993)
8. G. J. Schultz, Phys. Rev. 128, 178 (1962)
9. R. K. Asundi, J. D. Craggs and M. V. Kurepa, Proc. Phys, Sot. 82, 967 (1963)
10. H. H. Willard, L. L. Merritt, Jr., J. A. Dean and F. A. Settle, Jr., 'Instrumental Methods and Analysis', ch.29 (6th Ed., Van Nostand, New York) (1981)

## 7. Figure Captions

Fig. 1. Cross section for electron attachment to  $O_2$  as a function of electron energy. The cross section at the peak is  $1.34 \times 10^{-18} \text{ cm}^2$ .

Fig. 2. A schematic diagram of the experimental setup to demonstrate the resonant attachment method, where F are the filaments; G, cylindrical grid; T, stainless steel tube through which the oxygen molecules are introduced; EC, ion extraction cone;  $L_1$ -- $L_3$ , ion extraction lenses; A, entrance apertures; QMA, quadruple mass analyzer; CM, channel multiplier; and AMP, amplifier.

Fig. 3. A mass spectrum of dissociative electron attachment of  $O_2$ , showing a peak at  $m/e = 16$  corresponding to O.

Fig. 4. A sensitivity curve for detecting O from  $O_2$ , obtained by standard additions for mixing various concentrations of  $O_2$  in  $N_2$ . The solid line represents a least-squares fit to the data. The curve shows a measurement sensitivity down to  $1 \times 10^{-10}$  (O. 1 ppb).

Fig. 1

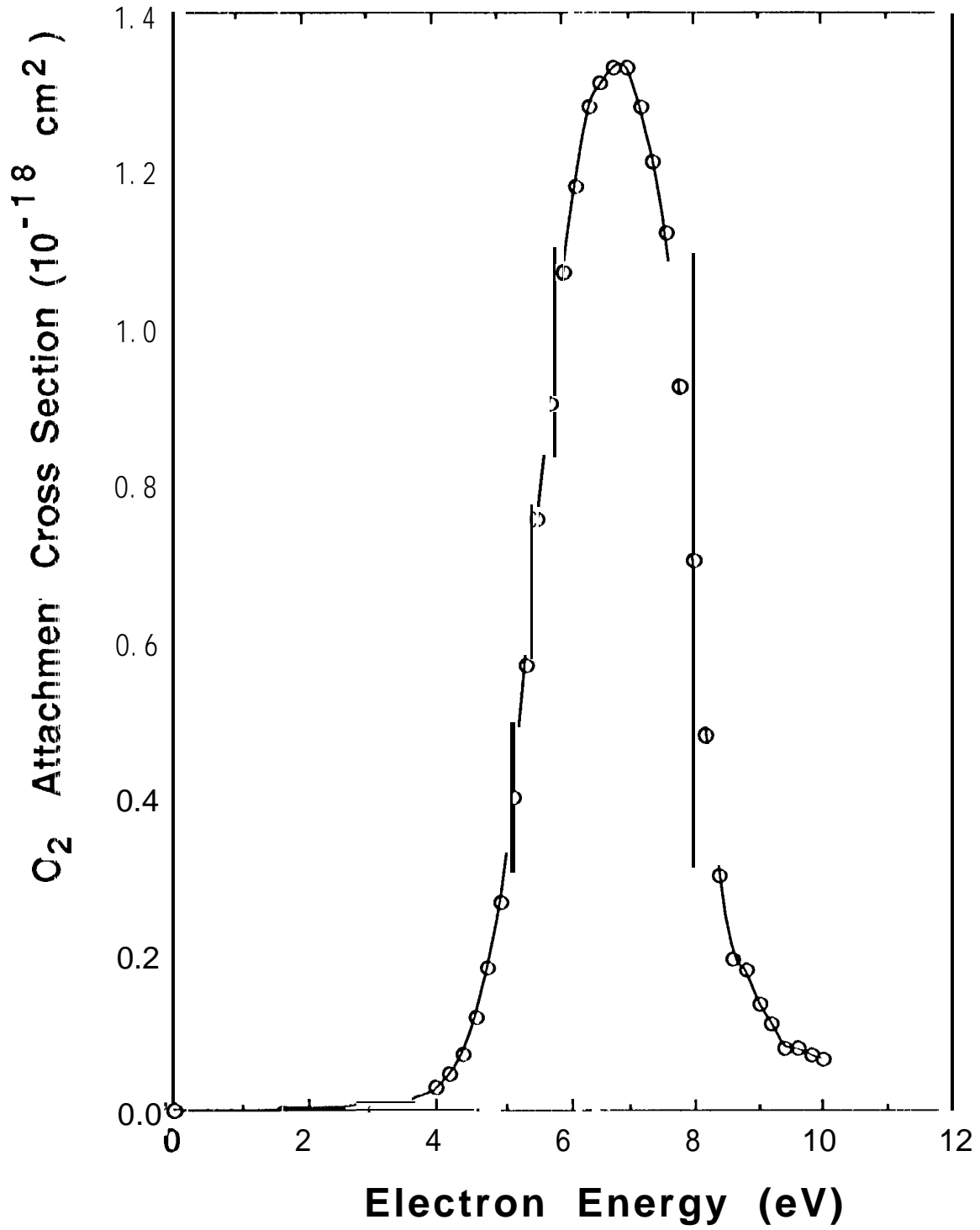


Fig. 2

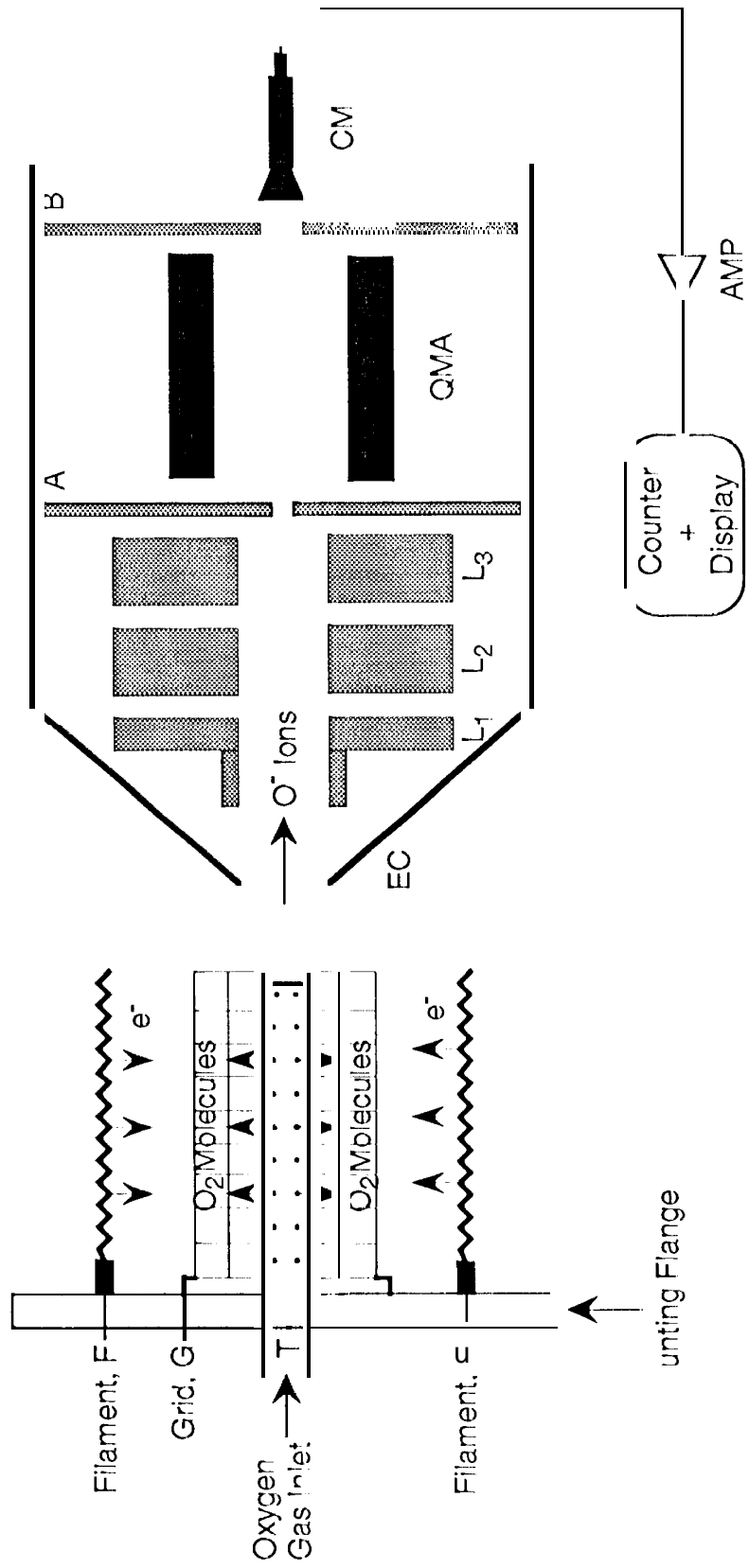
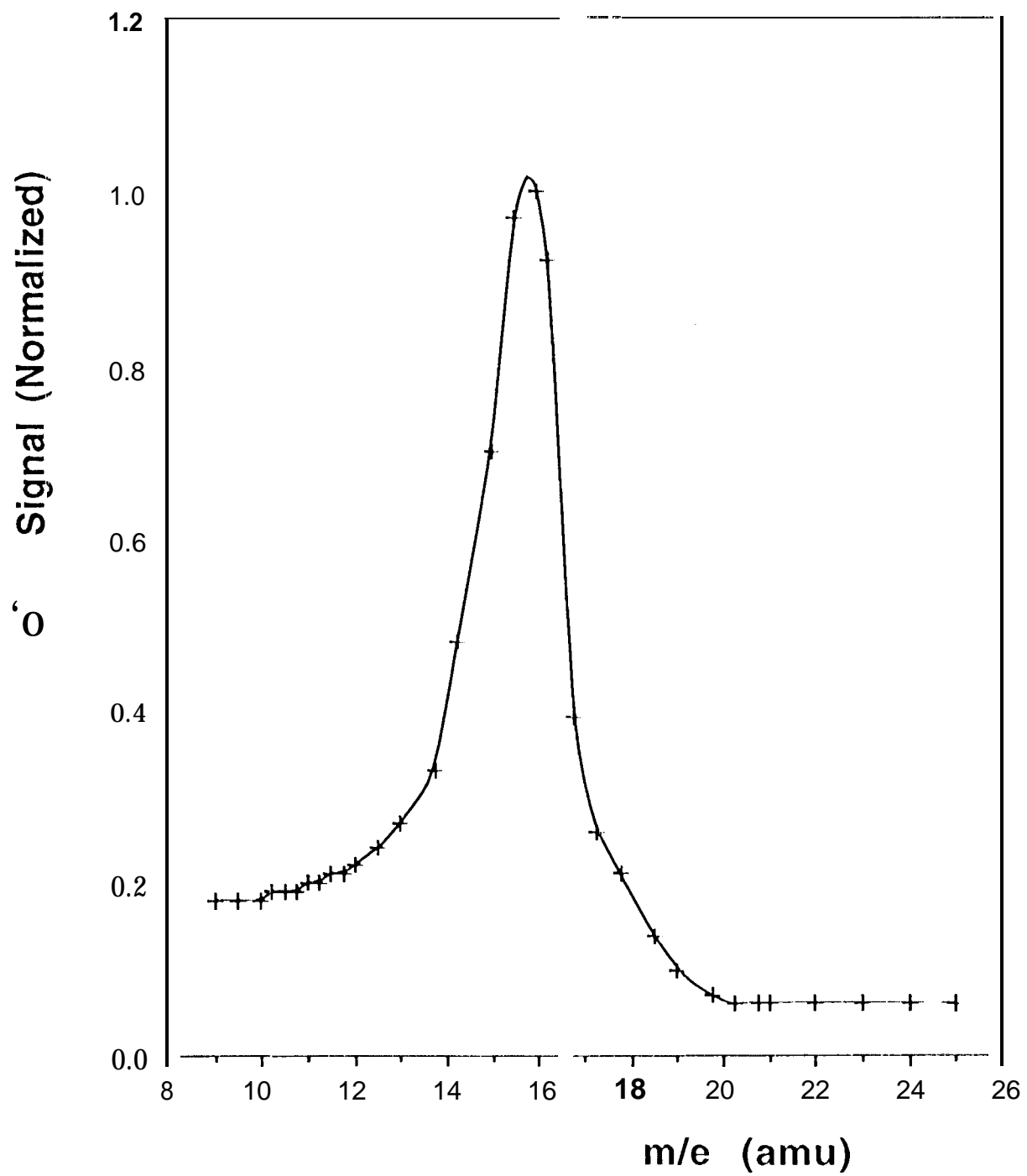


Fig. 3



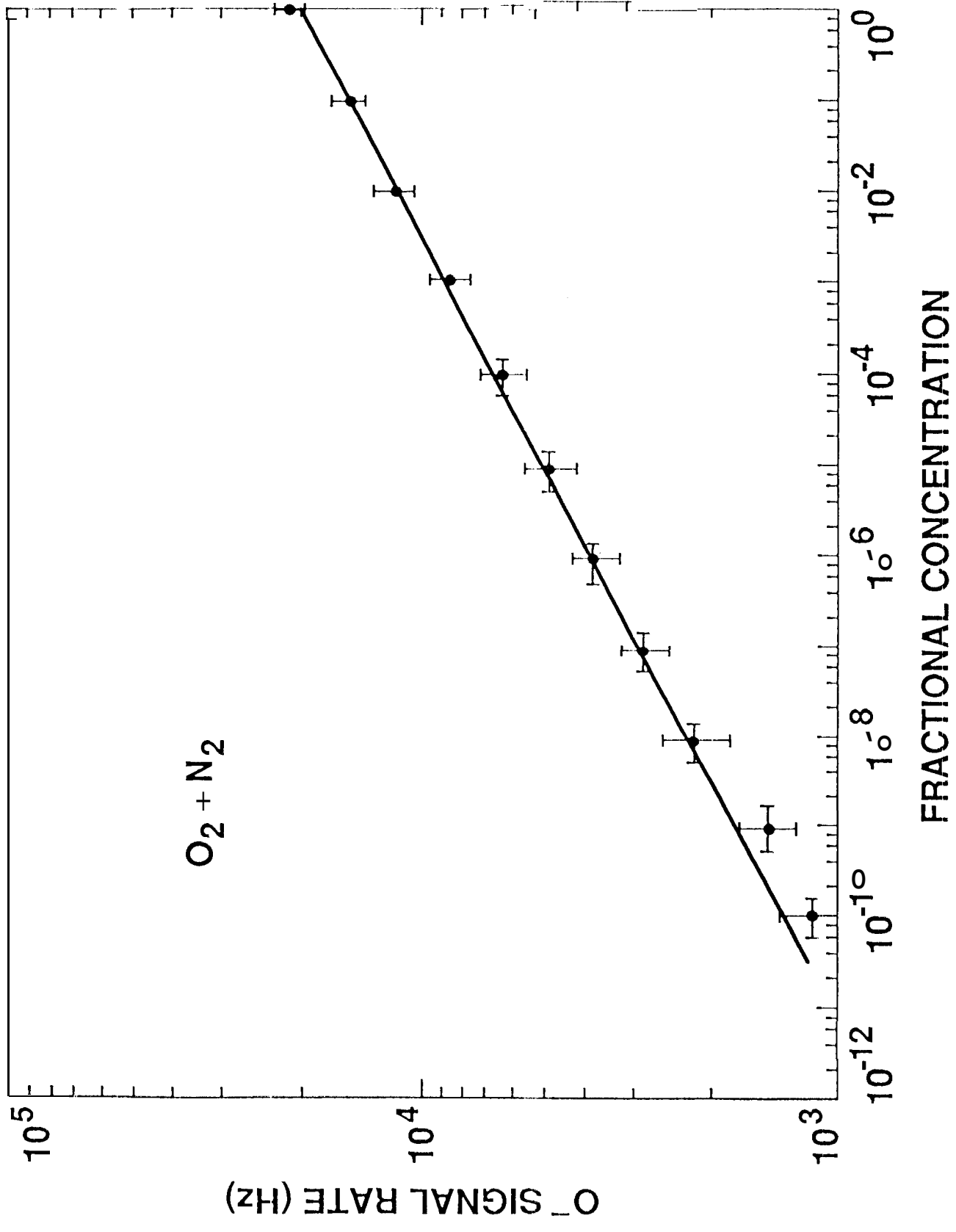


Fig 4